Specialty Journal of Pharmacognosy, Phytochemistry, and Biotechnology
ISSN: 3062-441X
2023, Volume 3, Page No: 164-182

Available online at: www.galaxypub.co/page/journals

Galaxy Publication

Galaxy Publication

Metabolic Reprogramming, Genomic Alterations, and Post-Translational Modifications in Pulmonary Hypertension and Cancer: Implications for Biomarkers and Therapeutic Targeting

Carlos Méndez[1], Javier Soto[1]*, Luis Calderón[1]

[1]Department of Pharmacognosy, Faculty of Pharmacy, University of Chile, Santiago, Chile.

***E-mail** ✉ javier.soto.pg@outlook.com

Received: 12 August 2023; **Revised:** 29 October 2023; **Accepted:** 06 November 2023

ABSTRACT

Pulmonary hypertension (PH) often results in right ventricular hypertrophy, contributing to higher mortality. This study investigates PH-associated metabolites and their influence on genomic alterations and post-translational modifications (PTMs) in cancer, while assessing the therapeutic potential of DHA and EPA in reducing oxidative stress and inflammation. Using Mendelian randomization on a cohort of 289,365 individuals, we explored the causal involvement of 1,400 metabolites in pulmonary hypertension. The potential anti-inflammatory and antioxidant actions of DHA and EPA were investigated in RAW 264.7 macrophages and multiple cancer cell lines (A549, HCT116, HepG2, LNCaP). We further characterized genomic alterations—including CNVs, DNA methylation patterns, tumor mutation burden (TMB), and post-translational modifications (PTMs)—and evaluated how DHA and EPA influence reactive oxygen species production and the proliferation of cancer cells. A total of 57 metabolites were found to be associated with pulmonary hypertension risk, and critical tumor-related pathways were investigated via promoter methylation analysis. DHA and EPA markedly lowered ROS levels and inflammatory markers in macrophages, suppressed proliferation across multiple cancer cell lines, and reduced the nuclear translocation of SUMOylated proteins under oxidative and inflammatory conditions. These results indicate a potential anticancer effect through modulation of stress-responsive nuclear signaling and regulation of cellular post-translational modifications. This study highlights alterations in metabolism and post-translational modifications in pulmonary hypertension and cancer, demonstrating that DHA and EPA can mitigate oxidative stress and inflammatory responses. The results underscore the potential of targeting these pathways for developing early biomarkers and therapeutic strategies, offering promising avenues to enhance disease management and patient outcomes."

Keywords: Pulmonary hypertension, Metabolomics, Cancer genomics, Biomarkers, Therapeutic targets, Drug

How to Cite This Article: Méndez C, Soto J, Calderón L. Metabolic Reprogramming, Genomic Alterations, and Post-Translational Modifications in Pulmonary Hypertension and Cancer: Implications for Biomarkers and Therapeutic Targeting. J Pharmacogn Phytochem Biotechnol. 2023;3:164-82. https://doi.org/10.51847/JAPK1fotYK

Introduction

Pulmonary hypertension (PH) is a life-threatening cardiovascular disorder characterized by persistently high pressure in the pulmonary arteries, often progressing to right ventricular failure. Beyond its hemodynamic impact, PH shares molecular and cellular features with other systemic diseases, most notably various cancers. Recent studies suggest that metabolic reprogramming plays a critical role in PH development, influencing disease progression through pathways that intersect with oxidative stress, inflammation, and vascular remodeling. This complexity is further amplified by comorbidities such as COVID-19, stroke, and pneumonia, which underscore the multifactorial nature of PH and its sensitivity to systemic metabolic and genetic factors. Specific metabolic disruptions, including altered plasma homocysteine levels and COPD-related pathways, have been linked to PH pathophysiology, highlighting potential therapeutic targets, particularly in vulnerable populations such as

postmenopausal diabetic women. Emerging nanotechnology-based approaches offer promising avenues for intervention, especially in the context of cancer treatment and drug delivery.

Metabolites do more than support cellular energy—they act as dynamic signaling molecules capable of modulating gene expression, protein function, and post-translational modifications (PTMs) such as phosphorylation, acetylation, and SUMOylation. These mechanisms are central to the interplay between oxidative stress, inflammation, and vascular dysfunction in PH. Hormonal regulation, for instance through estrogen receptor signaling in ovarian cancer, further connects systemic metabolism to vascular health. Tumor progression can also influence pulmonary vascular remodeling, suggesting bidirectional crosstalk between cancer and PH. Genomic studies reveal overlapping patterns between pan-cancer traits and PH, though many mechanistic details remain elusive. Investigations into m6A RNA methylation in cancer stem cells and epigenetic processes like epithelial-mesenchymal transition provide new perspectives on shared molecular drivers that may underlie both PH and cancer, offering potential targets for biomarker development and therapeutic intervention.

In cancer, genomic and epigenomic features such as copy number variations (CNVs), DNA methylation, tumor mutation burden (TMB), and post-translational modifications (PTMs) are intricately connected [1]. CNVs can alter gene dosage, influencing both gene expression and the prevalence of PTMs on affected proteins [2, 3]. DNA methylation further modulates PTMs by regulating the transcription of genes encoding enzymes responsible for these modifications [4, 5]. High TMB leads to the production of neoantigens that stimulate immune cell infiltration, often upregulating inflammation-related genes and indirectly affecting PTM landscapes [6]. PTMs themselves govern protein activity and stability, while also shaping the function of transcription factors and downstream gene networks [7]. Together, CNVs, DNA methylation, and PTMs form a complex regulatory network that influences tumor behavior and the immune microenvironment, providing critical insight for biomarker discovery and targeted therapy development.

Metabolites act as dynamic signaling molecules capable of regulating gene expression and protein function under both normal and disease conditions, including pulmonary hypertension (PH) [8]. Certain metabolites can directly modulate oxidative stress and inflammatory pathways in PH, frequently through PTM modifications such as phosphorylation, acetylation, or SUMOylation of key proteins [9]. Because PTMs respond to cellular metabolic status, fluctuations in metabolite levels can affect protein stability, activity, and localization, thereby influencing disease progression [10, 11]. These modifications may alter the function of transcription factors or structural proteins in pulmonary vascular cells, potentially exacerbating or mitigating PH. Furthermore, research into natural products in cancer, such as cervical cancer, points to metabolite-driven therapeutic strategies that could be translated to PH through shared metabolic and genetic pathways [12]. Overall, these observations support the hypothesis that metabolites, PH, and PTMs are tightly interconnected, with metabolic changes shaping PTM patterns and protein function. This framework provides a novel perspective for exploring PTMs as both biomarkers and therapeutic targets in PH.

Understanding the causal links between metabolites and pulmonary hypertension (PH), as well as their connections to genomic alterations in diverse cancers, remains a critical challenge. Current research often lacks detailed insight into how specific metabolites interact with genetic changes across different cancer types and the resulting implications for PH. Mendelian randomization has emerged as a powerful approach to clarify these relationships. When combined with bioinformatics and single-cell sequencing, it enables detailed characterization of immune responses across distinct tissue microenvironments, supporting the development of more precise, individualized therapies. Recent advances in high-throughput technologies have expanded the use of transcriptomics, metabolomics, and proteomics, enhancing disease diagnosis and treatment strategies [13-16]. This study seeks to address current knowledge gaps by investigating the causal effects of metabolites on PH and examining post-translational modification (PTM)-related genomic alterations across multiple cancer types. By exploring how metabolic fluctuations influence genetic and epigenetic changes in cancer, we aim to uncover the molecular pathways connecting PH and malignancy. These insights could identify novel therapeutic targets and diagnostic biomarkers, facilitating early detection and personalized treatment approaches. Integrating metabolic and genetic perspectives is essential to fully understand the complex interplay underlying PH and related diseases.

Materials and Methods

Integration analysis of exercise-related genes and metabolomics

The GENECARD database catalogs genes linked to exercise, offering information on their biological functions and interactions across diverse cellular processes. Leveraging the MetaboAnalyst platform, we integrate these gene datasets with metabolomic profiles to explore their combined roles in metabolic pathways.

Genomic features of cross-over genes in pan-cancer

For our pan-cancer analysis, we utilized DNA methylation and copy number variation (CNV) datasets from The Cancer Genome Atlas (TCGA). CNV data were extracted for genes shared across multiple tumor types, with each gene categorized as either amplified or deleted. The frequency of these alterations was then calculated for each tumor type. Promoter DNA methylation levels of the overlapping genes were assessed in both normal and tumor tissues using UALCAN (http://ualcan.path.uab.edu/analysis.html). The MethSurv database's "Gene Visualization" tool was employed to examine methylation patterns across different cancers. Additionally, mutation data in Mutation Annotation Format (MAF) were retrieved via the R package "TCGAbiolinks," and tumor mutation burden (TMB) was calculated using the "maftools" R package.

Pan-cancer GSEA enrichment analysis

Differential gene expression between tumor and normal samples from TCGA was assessed using the "limma" R package. Genes exhibiting significant expression changes were identified based on p-value thresholds and log2 fold change (log2FC) criteria. To explore the functional implications of these differences, Gene Set Enrichment Analysis (GSEA) was conducted using the "clusterProfiler" R package. The data were appropriately formatted for analysis, and the results were visualized to highlight key pathways and biologically relevant findings.

Tumor prognostic analysis

To investigate the prognostic significance of shared gene expressions, we analyzed TCGA patient data with a focus on overall survival (OS). Survival differences across cancer types were assessed using Kaplan-Meier curves and the log-rank test. Curve generation and visualization were performed with the "survival" and "survminer" R packages. Additionally, we applied the Cox proportional hazards model to explore the impact of FGA and NOTCH3 expression on OS in a pan-cancer cohort, with effect estimates and confidence intervals presented through forest plots using the "forestplot" R package.

Immune infiltration

We analyzed the infiltration of 22 immune cell types in tumor samples using marker data from CIBERSORTx (https://cibersortx.stanford.edu/) and the core CIBERSORT algorithm. The analysis was conducted through the CIBERSORT R script. To explore associations between individual gene expression and immune cell abundance across pan-cancer datasets, Spearman correlation analysis was performed, with results visualized using heatmaps. This approach provides a detailed assessment of the tumor microenvironment, offering insights into how immune cell populations contribute to cancer progression.

Methylation analysis

Our methylation analysis focuses on multiple regulatory regions, including TSS1500 (−1,500 to −200 bp upstream of the transcription start site), TSS200 (−200 bp upstream of the TSS), the first exon, and the 5′ untranslated region (5′UTR). For each sample, methylation levels are summarized using the median value. To assess the relationship between DNA methylation and gene expression, we applied Spearman's rank correlation, a non-parametric method that evaluates monotonic associations between variables regardless of their distribution. In this analysis, methylation levels serve as the independent variable, while gene expression levels are treated as the dependent variable. The strength and direction of the association are quantified using the Spearman correlation coefficient. Additionally, the Wilcoxon rank-sum test was employed to compare promoter methylation distributions between tumor and normal tissue group

Gene set enrichment analysis and GSVA analysiss.

Gene Ontology (GO) enrichment analysis was performed on the selected gene sets using the "clusterProfiler" R package, which was also employed to conduct Kyoto Encyclopedia of Genes and Genomes (KEGG) pathway enrichment analysis. To quantify pathway activity, Gene Set Variation Analysis (GSVA) was applied using four approaches: zscore, gsva, ssgsea, and plage. Except for the zscore method, results from the other approaches were

converted to unitless Z-scores $(x-\mu)/(x-\mu)/\sigma$ to standardize values across tumor samples. Differences between tumor and normal tissues were evaluated using the Wilcoxon rank-sum test, and results were visualized through boxplots generated with the ggplot2 package.

RAW 264.7 cell line

The RAW 264.7 macrophage cell line was obtained from the Shanghai Cell Bank, Chinese Academy of Sciences. Cells were maintained in RPMI-1640 medium (Gibco Invitrogen, San Diego, CA, USA) supplemented with 10% fetal bovine serum (Gibco BRL, Grand Island, NY, USA), 100 U/mL penicillin, and 0.1 mg/mL streptomycin, under standard conditions of 37°C, 95% humidity, and 5% CO_2. Docosahexaenoic acid (DHA) was prepared as a 1 mM stock solution in dimethyl sulfoxide (DMSO) and stored at −20°C. For experimental treatments, the stock solution was diluted with DMSO to achieve a final concentration of 2 μM DHA or eicosapentaenoic acid (EPA), and cells were exposed for 48 hours. DHA (≥99% purity; D2534) and the fatty acid standard mixture were purchased from Sigma (St. Louis, MO, USA), while EPA was obtained from Sigma-Aldrich (St. Louis, MO, USA).

Cell culture and colony formation assay

The LNCaP (prostate), HepG2 (liver), A549 (lung adenocarcinoma), and HCT116 (colorectal) cell lines were maintained in DMEM supplemented with 10% FBS and 1% penicillin-streptomycin under standard culture conditions at 37°C in a 5% CO_2 humidified incubator. Media were replenished every 2–3 days, and cells were passaged using 0.25% trypsin-EDTA upon reaching 80–90% confluence. Cell line authentication was performed prior to experiments to ensure experimental validity. For colony formation assays, cells were plated in 6-well plates at 500–1,000 cells per well and incubated overnight to allow attachment. Cultures were maintained under standard conditions, with fresh medium provided every 3–4 days. After 10–14 days, colonies became visible and were fixed in 4% paraformaldehyde for 15 minutes, followed by staining with 0.5% crystal violet for 20 minutes. Plates were rinsed with tap water and air-dried. Colonies containing more than 50 cells were counted under a microscope, and the colony formation efficiency was calculated as the number of colonies relative to the number of cells initially plated.

Inhibition of reactive oxygen species (ROS) production

RAW 264.7 cells were prepared at a density of 2.5×10^5 cells/mL. Each well received luminol, a compound that amplifies light signals, along with zymosan to trigger reactive oxygen species (ROS) production. The resulting chemiluminescence, reflecting ROS generation, was subsequently measured.

Immunofluorescence detection

Immunofluorescence staining was carried out following established protocols. Cells were first fixed in 4% paraformaldehyde (PFA) for 15 minutes, then blocked for 1 hour to prevent non-specific binding. Samples were incubated overnight at 4°C with the primary antibody. On the following day, cells were returned to room temperature (≈25°C) and incubated with a fluorescently conjugated secondary antibody for 1 hour. After washing with PBS, coverslips were mounted using an anti-fade medium containing DAPI (Abcam). Images were captured using fluorescence microscopy.

Statistical analysis

A P-value below 0.05 was considered indicative of statistical significance, confirming the reliability and validity of our findings related to metabolites and pulmonary hypertension. Data are presented as mean ± standard error.

Results and Discussion

Causal relationship between metabolites and the risk of pulmonary hypertension

To investigate whether specific metabolites influence pulmonary hypertension (PH), we applied a two-sample Mendelian Randomization (MR) framework. The MR Egger intercept test showed no evidence of horizontal pleiotropy (all $p > 0.05$), indicating the reliability of our genetic instruments. Sensitivity analysis using a leave-one-out jackknife approach is presented in **Figure 1**. In total, 57 metabolites demonstrated a significant causal relationship with PH at $P < 0.01$. Notably, Glucuronide of piperine ($P = 0.030$, OR = 1.316, 95% CI = 1.026–

1.689), N-lactoyl valine (P = 0.034, OR = 2.029, 95% CI = 1.052–3.911), and N-stearoyl-sphingadienine (d18:2/18:0) (P = 0.007, OR = 1.570, 95% CI = 1.126–2.189) were associated with increased risk of PH. In contrast, Cerotoylcarnitine (C26) (P = 0.027, OR = 0.688, 95% CI = 0.493–0.959), Docosatrienoate (22:3n6) (P = 0.041, OR = 0.642, 95% CI = 0.420–0.982), and 5-dodecenoylcarnitine (C12:1) (P = 0.036, OR = 0.545, 95% CI = 0.309–0.962) exhibited protective effects. Reverse MR analyses examined whether PH influenced metabolite levels, revealing a negative correlation with S-methylcysteine (P = 0.045, OR = 1.014, 95% CI = 1.000–1.028). The MR Forest Plot illustrates the odds ratios (ORs) and 95% confidence intervals (CIs), highlighting significant associations when the CI does not cross 1.

To strengthen causal inference, multiple MR methods were employed, including Inverse-Variance Weighted (IVW), MR Egger, weighted median, weighted mode, and simple mode analyses using genetic instruments from GWAS datasets. IVW combined estimates across instruments, MR Egger controlled for potential directional pleiotropy, and the weighted median provided robust results even if up to 50% of instruments were invalid. Collectively, these analyses indicate significant causal associations between certain metabolites and PH, offering potential biomarkers and therapeutic targets for disease management.

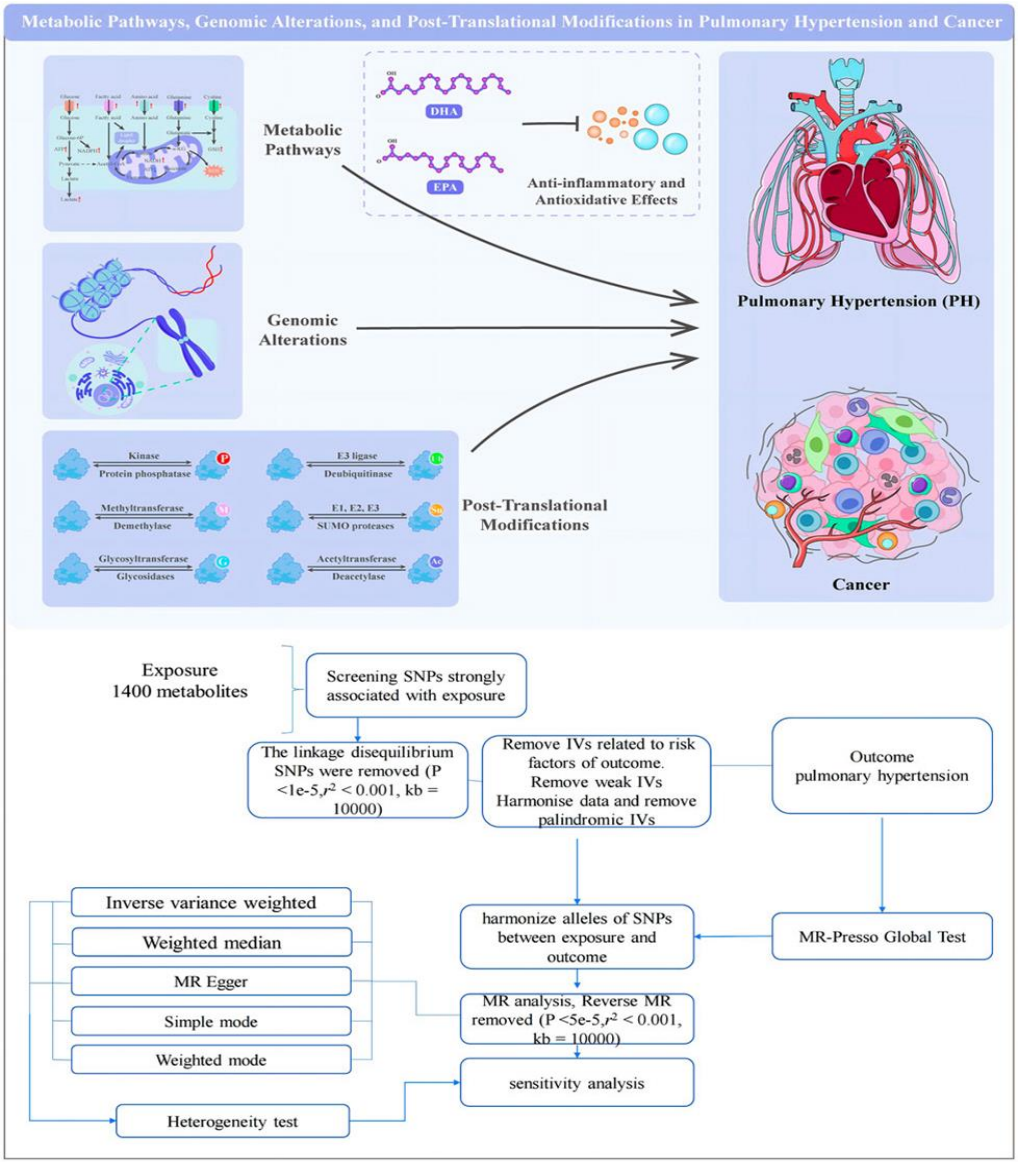

Figure 1. Workflow of Mendelian Randomization Analysis for Pulmonary Hypertension.

The diagram illustrates the systematic strategy used to assess the relationship between 1,400 metabolites and pulmonary hypertension (PH). The process begins with the selection of metabolites, followed by identification of single nucleotide polymorphisms (SNPs) strongly linked to each metabolite. SNPs in linkage disequilibrium (r^2 >

0.0001, $p < 1\times10^{-5}$) located within 10,000 base pairs are excluded. Instrumental variables (IVs) associated with potential confounders or lacking adequate strength are removed. The remaining data are standardized, and palindromic IVs are discarded to ensure consistent alignment of alleles between exposure and outcome SNPs. PH is designated as the outcome variable. SNPs are harmonized between the exposure and outcome datasets. Reverse MR is performed, and MR analysis is conducted using independent IVs with $p < 5\times10^{-5}$, $r^2 < 0.001$, and a distance threshold of 10,000 bp. Multiple MR methods—including Inverse-Variance Weighted (IVW), Weighted Median, MR Egger, Simple Mode, and Weighted Mode—are applied to assess causality. Heterogeneity tests evaluate the consistency of effects across methods, while MR-PRESSO Global Test identifies and corrects for horizontal pleiotropy. Sensitivity analyses are also conducted to confirm the robustness of the findings. This comprehensive workflow ensures that the associations identified between metabolites and PH are reliable and minimally influenced by confounding or pleiotropic effects.

Identification of metabolic pathways and exercise-related genes associated with pulmonary hypertension

Investigation of metabolic pathways and exercise-linked genes offered important insights into potential targets for pulmonary hypertension (PH) therapy. **Figure 2a** presents the 25 most enriched pathways derived from metabolomic profiling of PH patients using MetaboAnalyst 6.0. Pathways are ranked by statistical significance (p-value, left panel) and enrichment ratio (right panel). Notable pathways associated with PH included D-Arginine and D-Ornithine metabolism, starch and sucrose metabolism, and galactose metabolism. Dot size and color indicate enrichment magnitude and statistical relevance, respectively, with higher enrichment and stronger significance highlighted in red. These findings suggest that disturbances in amino acid and carbohydrate metabolism may play key roles in PH development and could provide avenues for metabolic interventions. **Figure 2b** depicts a network of exercise-related genes and their links to various diseases, constructed using GeneCards data. Genes such as IL6, IL1B, COL1A1, COL5A1, IL10, IFNG, PRL, MPO, ACE, CCL2, REN, and F2 were associated with conditions including inflammatory bowel disease, diabetes, rheumatoid arthritis, and Parkinson's disease. These genes are central to inflammation, immune regulation, and metabolic processes. The network highlights their potential involvement in the physiological response to exercise and suggests a role in modulating metabolic and immune dysregulation in PH. This integrated analysis of pathways and genes provides a basis for developing exercise-centered strategies to mitigate PH-related metabolic and immune alterations.

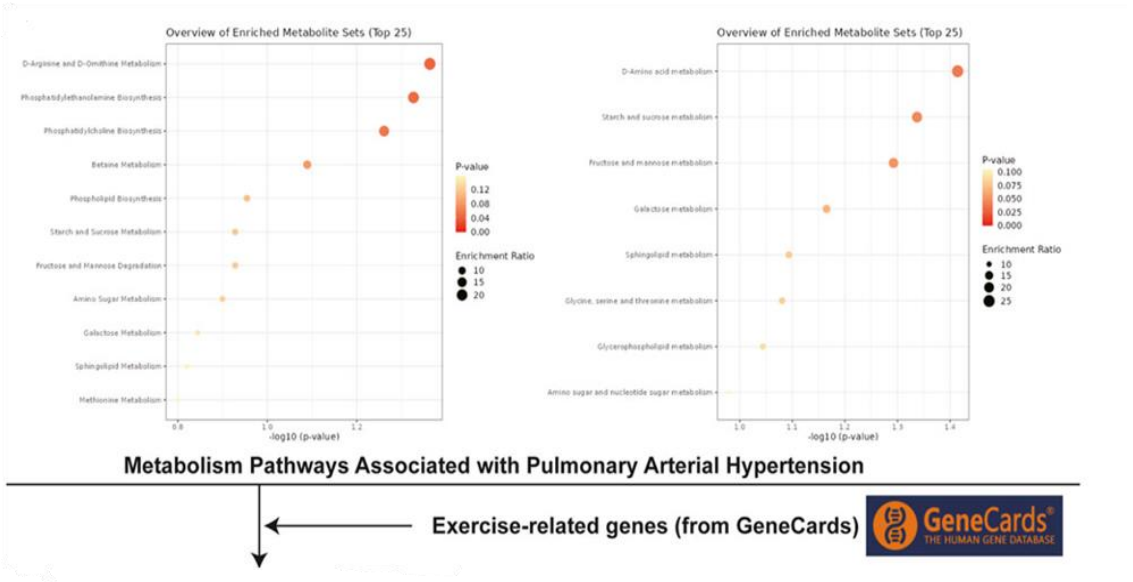

a)

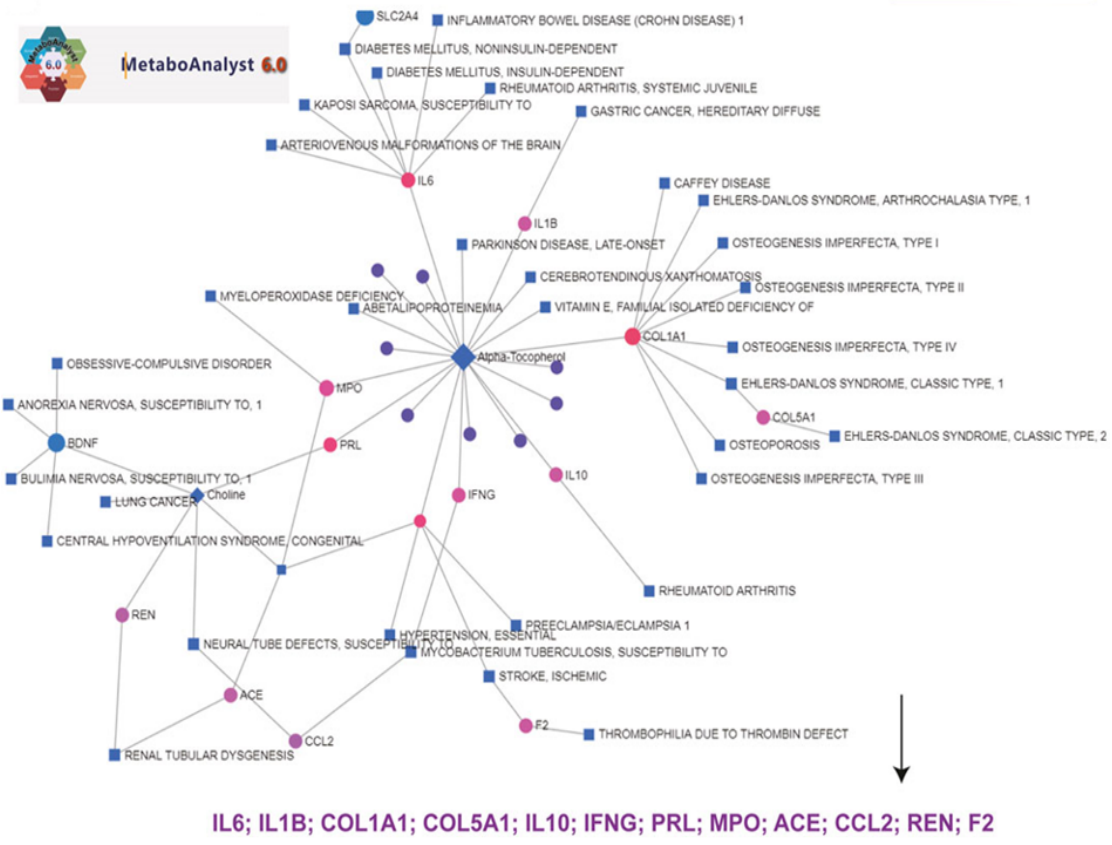

b)

Figure 2. Metabolic Pathways and Exercise-Associated Genes in Pulmonary Hypertension. (a) Top 25 metabolic pathways significantly linked to pulmonary hypertension (PH) are displayed. The left panel ranks pathways according to their p-values, while the right panel highlights those with higher enrichment ratios. Each dot represents an individual pathway, with color indicating statistical significance (red = more significant) and size representing the enrichment ratio. Analysis was performed using the MetaboAnalyst 6.0 platform based on metabolomics data from PH patients. (b) Network diagram showing connections between exercise-associated genes and various diseases.

Genes including IL6, IL1β, COL1A1, COL5A1, IL10, IFNG, PRL, MPO, ACE, CCL2, REN, and F2 were mapped using the GeneCards database. Nodes correspond to genes, edges indicate associations with diseases, and node size and color reflect the strength and significance of the connections. This visualization highlights the involvement of these genes in multiple conditions, including inflammatory bowel disease, diabetes, rheumatoid arthritis, and Parkinson's disease, emphasizing their relevance to both exercise physiology and pulmonary hypertension.

Prognostic significance of overlapping gene expression in various cancers

This study explored the prognostic roles of 12 genes (ACE, CCL2, COL1A1, COL5A1, F2, IFNG, IL1B, IL6, IL10, MPO, PRL, and REN) across multiple cancer types by analyzing their impact on overall survival (OS). Hazard ratios (HRs) with 95% confidence intervals (CIs) were calculated to assess whether higher or lower expression levels corresponded to better or worse patient outcomes.

ACE showed protective effects in kidney renal clear cell carcinoma (KIRC) and mesothelioma (MESO), but conversely, high ACE expression appeared detrimental in uterine carcinosarcoma (UCS). Elevated CCL2 levels were associated with poorer prognosis in kidney renal papillary cell carcinoma (KIRP) and low-grade glioma (LGG). COL1A1 expression correlated with increased risk in breast invasive carcinoma (BRCA), head and neck squamous cell carcinoma (HNSC), and stomach adenocarcinoma (STAD), while demonstrating protective effects in kidney chromophobe (KICH). Similarly, COL5A1 expression was linked to adverse outcomes in liver hepatocellular carcinoma (LIHC) and lung adenocarcinoma (LUAD) but appeared beneficial in KIRC.

F2 generally showed protective trends, although it was associated with higher risk in KIRC, BLCA, SARC, and LGG. IFNG expression appeared favorable in esophageal carcinoma (ESCA) and KIRC but unfavorable in BRCA. IL1B was protective in KIRC and BRCA but corresponded to worse prognosis in STAD and skin cutaneous melanoma (SKCM), reflecting its complex influence in tumor-related inflammation. IL6 exhibited a similar dual pattern, being protective in KIRC but indicating poor outcomes in lung squamous cell carcinoma (LUSC) and BLCA.

IL10 was linked to higher risk in KIRP and pancreatic adenocarcinoma (PAAD) yet showed protective tendencies in LUSC. MPO expression correlated with unfavorable prognosis in LIHC and LUSC but protective effects in BLCA. PRL was associated with increased risk in COAD and BRCA but improved outcomes in KIRC. REN demonstrated protective effects in KIRC and KIRP, while higher expression increased risk in LGG and UCS. Overall, these findings highlight the diverse, context-dependent roles of these genes in cancer prognosis, suggesting their potential as biomarkers for patient stratification

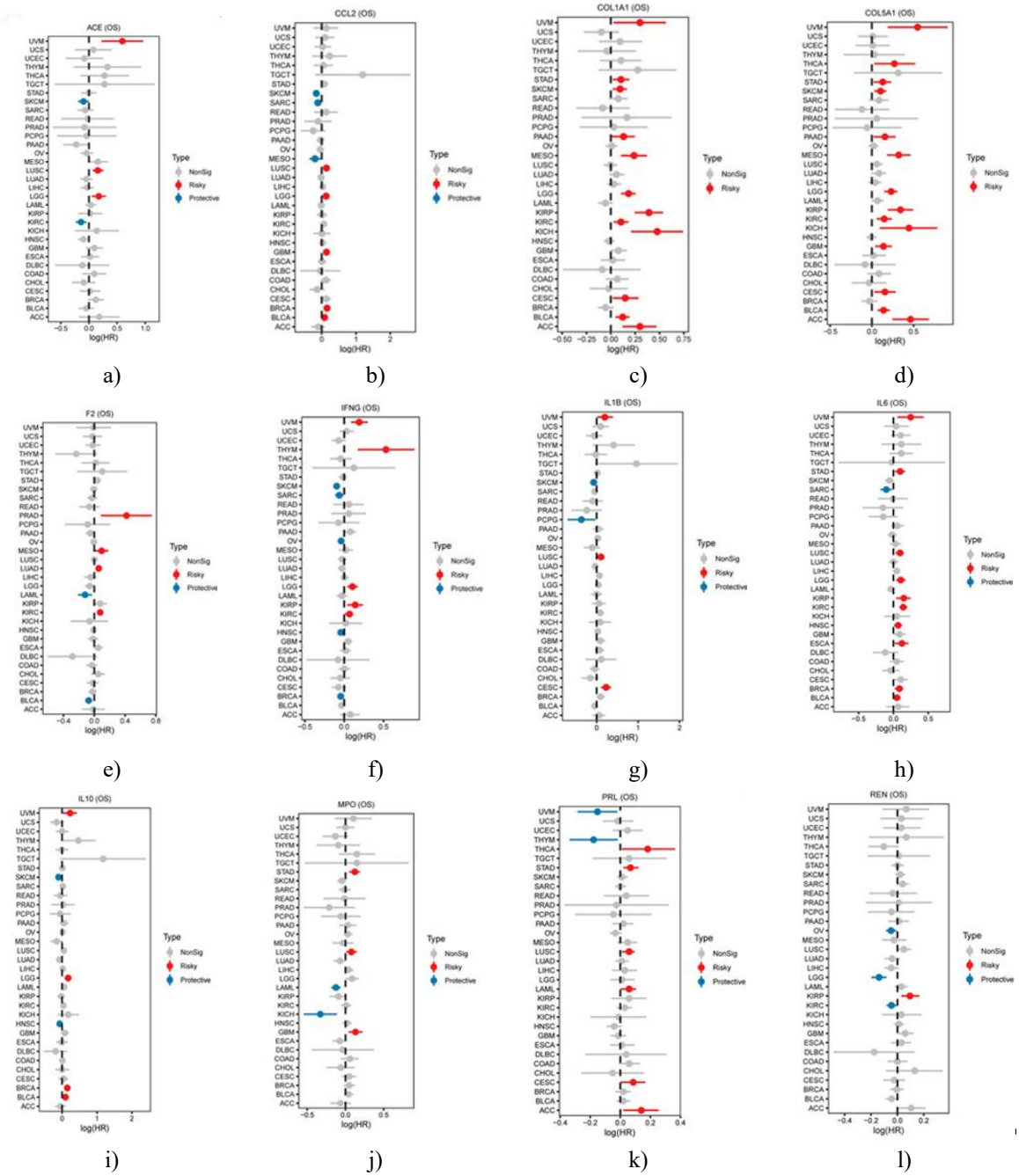

Figure 3. Prognostic Impact of Overlapping Gene Expression Across Cancers.

Figure 3 presents forest plots that show hazard ratios (HRs) and 95% confidence intervals (CIs) for 12 overlapping genes (ACE, CCL2, COL1A1, COL5A1, F2, IFNG, IL1β, IL6, IL10, MPO, PRL, and REN) in various tumor types. These plots illustrate how the expression levels of these genes are associated with overall survival (OS), indicating whether higher expression confers a survival advantage or disadvantage. ACE (OS): Higher ACE levels were linked to improved survival in KIRC and MESO, but worse outcomes in UCS. CCL2 (OS): Increased CCL2 expression predicted poorer prognosis in KIRP and LGG. COL1A1 (OS): Elevated COL1A1 was detrimental in BRCA, HNSC, and STAD, whereas it appeared protective in KICH. COL5A1 (OS): Higher COL5A1 levels were associated with higher risk in LIHC and LUAD but indicated better survival in KIRC. F2 (OS): F2 expression tended to be beneficial in KIRC and BLCA but unfavorable in SARC and LGG. IFNG (OS): IFNG expression correlated with improved outcomes in ESCA and KIRC, but was linked to worse prognosis in BRCA. IL1β (OS): Higher IL1B expression was favorable in KIRC and BRCA but associated with increased risk in STAD and SKCM. IL6 (OS): Elevated IL6 predicted poorer survival in LUSC and BLCA, yet had protective effects in KIRC. IL10 (OS): IL10 overexpression was associated with worse outcomes in KIRP and PAAD but improved prognosis in LUSC. MPO (OS): MPO levels were risky in LIHC and LUSC but protective in BLCA. PRL (OS): High PRL expression corresponded to higher risk in COAD and BRCA, while being beneficial in KIRC. REN (OS): REN expression conferred a survival advantage in KIRC and KIRP but was linked to poorer outcomes in LGG and UCS.

Analysis of copy number variation, methylation, and TMB of overlapping genes in pan-cancer

Next, we investigated the functional features of the overlapping genes in pan-cancer by analyzing copy number variation (CNV), DNA methylation, and tumor mutational burden (TMB). **Figure 4a** depicts the CNV landscape of these genes across 20 cancer types. Each bar reflects gene-specific CNV alterations across cancers, with different colors representing individual tumor types. Notably, COL1A1 and COL5A1 frequently exhibited CNV gains in BRCA and STAD, while ACE and IFNG showed CNV losses in KIRC and LUAD. **Figure 4b** shows the differential expression of these genes across tumors. IL6 and IL10 were markedly upregulated in cancers such as PAAD and LIHC, suggesting their involvement in tumor progression and inflammatory responses. **Figure 4c** examines the correlation between CNV and gene expression. Genes like COL1A1 and COL5A1 demonstrated strong positive correlations in BRCA and STAD, indicating that CNV gains can drive higher gene expression. In contrast, IFNG showed negative correlations in LUAD, suggesting that CNV losses may reduce its expression in certain cancers. **Figure 4d** explores the relationship between promoter methylation and gene expression. Hypermethylation of ACE and F2 was associated with lower expression in LUAD and KIRC, highlighting epigenetic silencing. Conversely, hypomethylation of IL1B and IL6 in COAD and BRCA corresponded with increased expression, implying promoter demethylation could activate oncogenic pathways**. Figure 4e** presents the association between TMB and gene expression. IL6 and MPO expression positively correlated with TMB in highly mutated tumors like LUSC and ESCA, suggesting that mutation burden may drive inflammatory gene upregulation. Meanwhile, REN and PRL showed negative correlations with TMB in KIRC, indicating potential suppression in tumors with high mutation loads. **Figure 4f** shows δ-values of promoter methylation comparing tumors and normal tissues. COL5A1 and MPO were significantly hypermethylated in STAD and BRCA tumors, correlating with reduced expression, whereas IL10 and IFNG were hypomethylated in PAAD and LUSC, corresponding with elevated mRNA levels and a potential pro-tumorigenic role. Finally, Gene Set Enrichment Analysis (GSEA) was performed across multiple cancers—including CESC, GBM, HNSC, KIRC, LAML, LIHC, LUAD, LUSC, OV, PAAD, PRAD, READ, SKCM, STAD, TGCT, and UVM. Thousands of pathways were examined, encompassing essential cellular processes such as xenobiotic metabolism, WNT/β-catenin signaling, unfolded protein response, and epithelial-to-mesenchymal transition (EMT), among others.

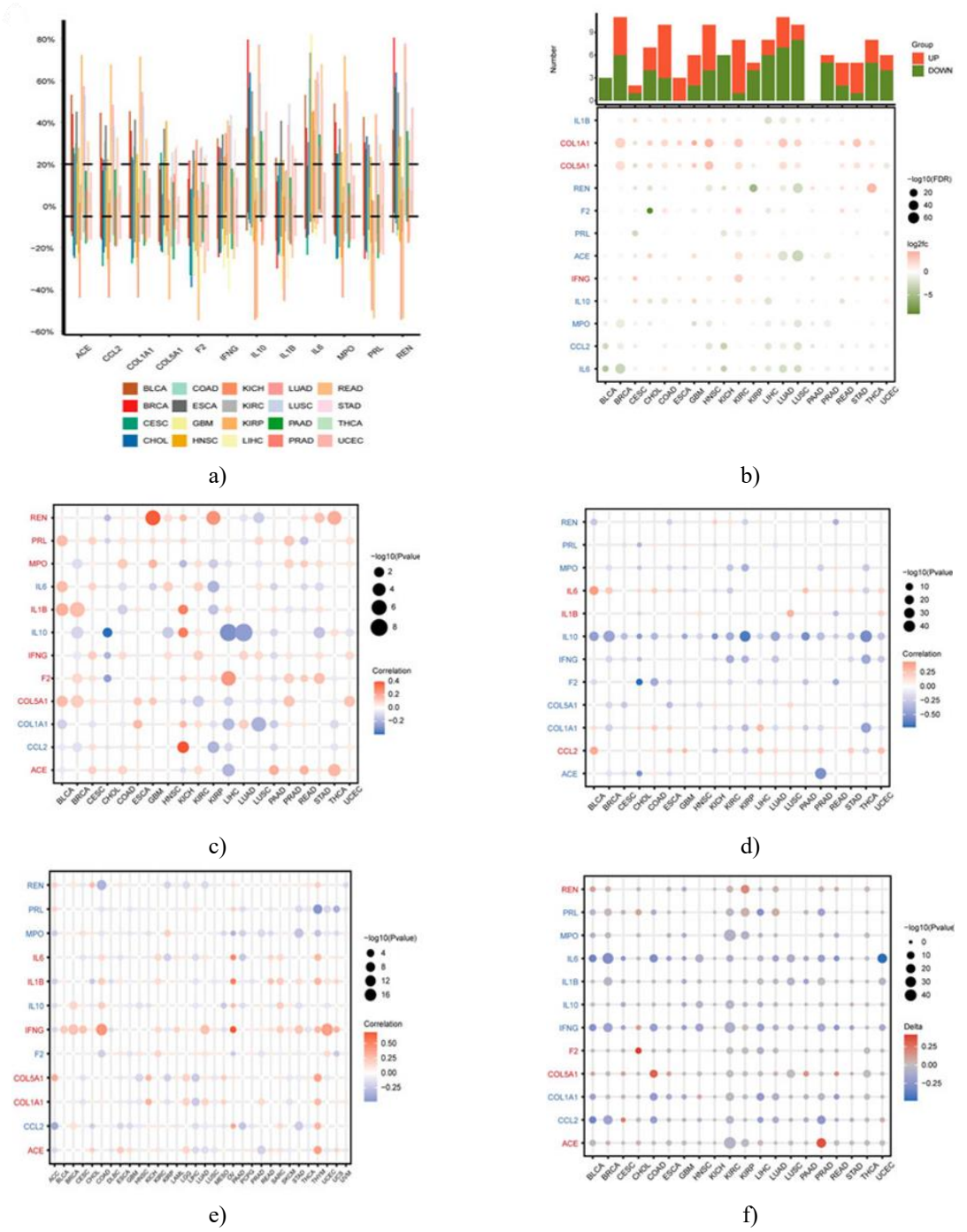

Figure 4. Pan-Cancer Analysis of Copy Number Variation, Methylation, and Tumor Mutational Burden of Overlapping Genes. (a) Distribution of copy number variation (CNV) among overlapping genes across 20 cancer types. Each bar represents CNV differences for a given gene across cancers, with colors distinguishing individual tumor types (b) Differential expression of overlapping genes across multiple cancers. The top bar chart indicates the number of genes upregulated (red) or downregulated (green) in each tumor type. The lower dot plot depicts expression levels, where dot size reflects statistical significance (-log10 FDR) and color corresponds to log2 fold change. (c) Correlation between gene dosage and expression. The dot plot shows color-coded correlation coefficients between CNV and gene expression across different cancers. (d) Impact of promoter methylation on gene expression. Correlation coefficients are color-coded to indicate how changes in promoter methylation affect gene expression in various tumors.(e) Relationship between tumor mutational burden (TMB) and gene expression. The dot plot presents color-coded correlation coefficients, with dot size representing the significance (-log10 p-value), highlighting genes whose expression is influenced by mutation load. (f) δ-values of promoter methylation in tumor versus normal tissues. This plot

shows the differences in methylation (δ-values) between tumors and normal samples, with dot size indicating statistical significance (-log10 p-value).

Correlation of overlapping gene expression with immune cell infiltration and minor allele frequency across cancers

This study provides a comprehensive pan-cancer exploration of the connections between key overlapping gene expression, immune cell infiltration, tumor mutational burden (TMB), and mutation allele frequency (MAF), highlighting their functional significance across tumor types. We employed CIBERSORT to generate heatmaps, radial plots, and MAF maps to systematically investigate these relationships.

Heatmaps in **Figures 5a–5j** illustrate how the expression of genes such as ACE, CCL2, COL1A1, COL5A1, F2, IFNG, IL1B, IL6, IL10, MPO, PRL, and REN correlates with the presence of various immune cells, including B cells, CD8+ T cells, regulatory T cells, NK cells, macrophages, immature and activated dendritic cells, and mast cells. These patterns underscore the potential influence of these genes on shaping the tumor immune microenvironment.

Radial plots **(Figure 5k)** revealed a bimodal expression pattern of TMB-associated genes across cancers, suggesting that these genes may play regulatory roles in the accumulation of mutations. Meanwhile, MAF heatmaps **(Figure 5l)** highlighted differences in mutation frequencies among cancers, reflecting tumor heterogeneity and the diverse selective pressures acting on these genes during tumor development.

Together, these analyses shed light on the genetic and immunological features of tumors, uncover potential biomarkers for cancer prognosis and detection, and provide insight into the molecular mechanisms that could drive tumor progression.

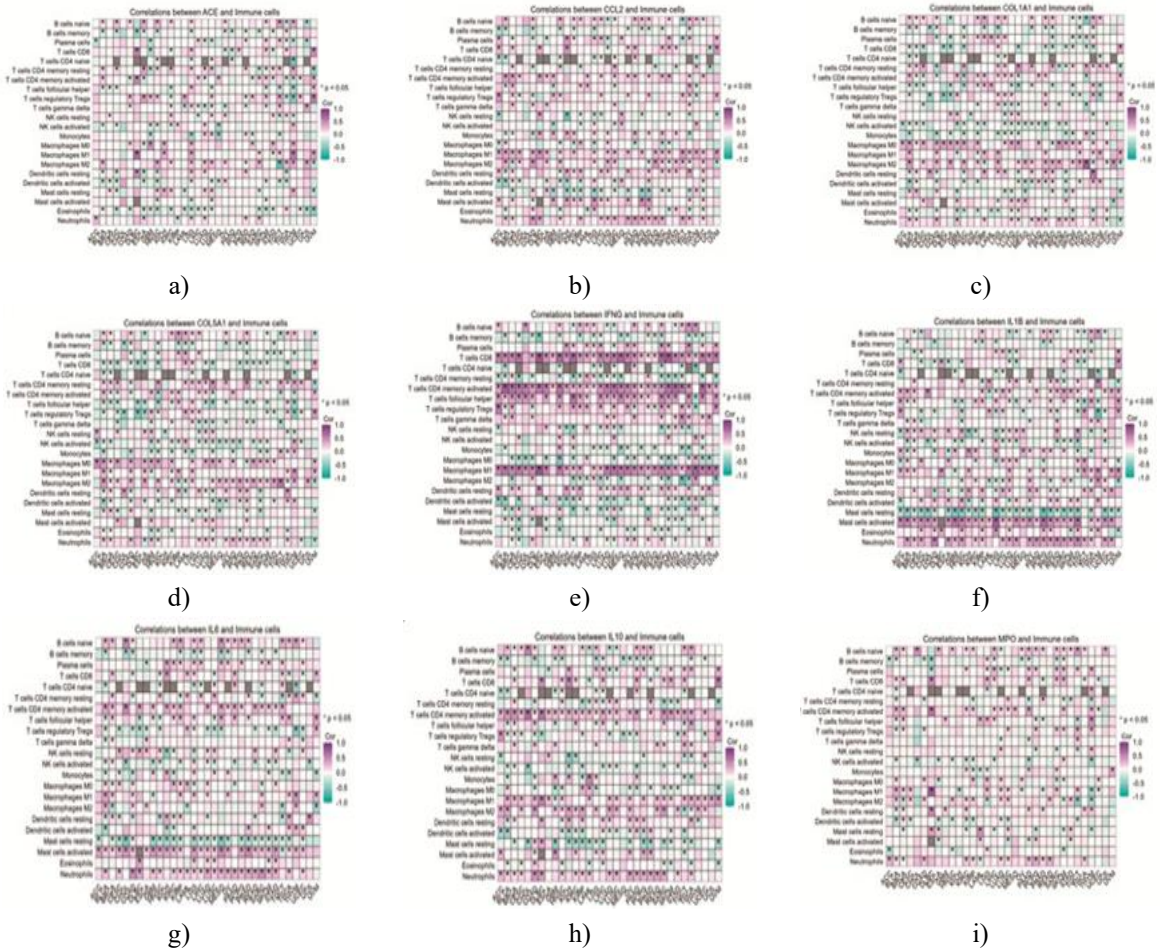

a) b) c)

d) e) f)

g) h) i)

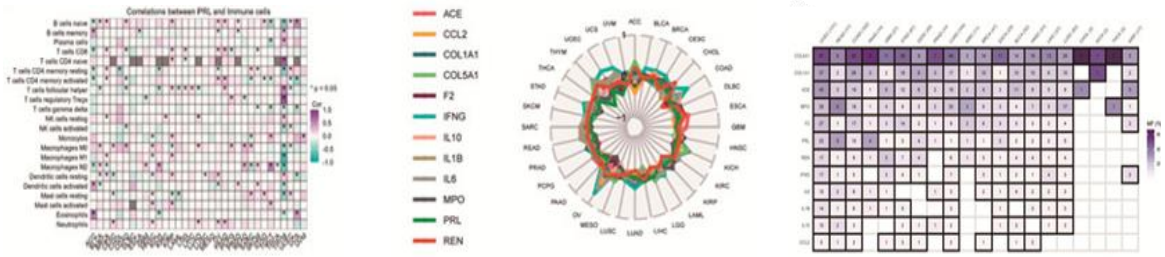

j) k) l)

Figure 5. Pan-Cancer Analysis of Overlapping Genes, Immune Infiltration, TMB, and MAF.
(a–j) Correlation heatmaps depicting how the expression of twelve key genes (ACE, CCL2, COL1A1, COL5A1, F2, IFNG, IL1β, IL6, IL10, MPO, PRL, and REN) relates to immune cell abundance across multiple cancers. Each panel focuses on one gene and displays its associations with diverse immune populations, including B cells, CD8+ and CD4+ T cells, NK cells, macrophages, dendritic cells, and mast cells. The color gradient represents the strength and direction of correlation (purple for positive, green for negative), and the size of each square reflects statistical significance, with larger squares denoting $p < 0.05$.
(k) Radial plots illustrating TMB-associated expression patterns of the same genes across cancers. The plot's circular layout maps different cancer types along the circumference, while the colored lines trace gene expression trends in relation to TMB, standardized for cross-comparison. Correlations were quantified using Pearson coefficients.
(l) Heatmap showing minor allele frequencies (MAF) for overlapping genes across cancer types. Each cell corresponds to a specific gene-cancer pair, with deeper colors indicating higher allele frequency. Chi-square tests were applied to evaluate the significance of these variations.

Pathway analysis in various tumors

A combined evaluation of promoter methylation, its impact on gene expression, and pathway-level activity can provide important insights into mechanisms of tumor development across cancers. **Figure 6a** shows heatmaps of promoter methylation across multiple tumor types, where red indicates markedly higher methylation in tumors compared to normal tissue, and blue indicates lower methylation levels. In **Figure 6b**, promoter methylation is plotted against mRNA expression, with red highlighting positive correlations and blue indicating inverse relationships, emphasizing the complex regulatory effects of methylation on gene expression. Boxplots in **Figures 6c–6f** display Z-scores for pathway activity in tumor versus normal tissues across various cancers. The Wilcoxon Rank Sum Test was used to evaluate statistical significance, revealing notable differences in pathway activity between tumor and normal samples, with specific patterns varying by cancer type. **Figure 6g** presents KEGG pathway enrichment as a scatter plot. Dot size reflects the proportion of genes enriched in each pathway, while the color gradient from yellow to blue represents significance levels, pinpointing key pathways that are highly activated in tumors and may serve as potential therapeutic targets Finally, **Figure 6h** shows a radial plot summarizing GO enrichment analysis, providing a visual overview of the biological processes most affected in tumors.

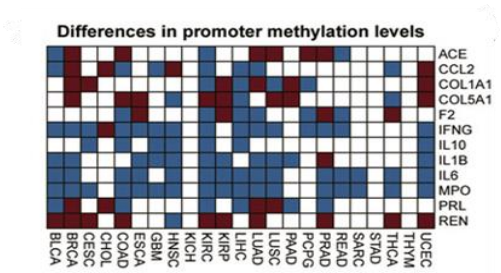

a)

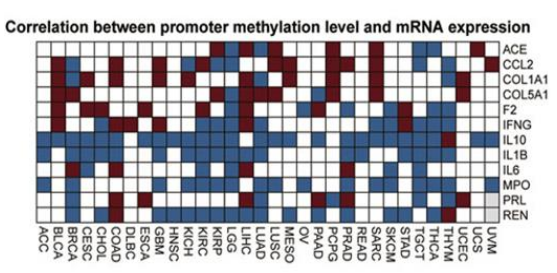

b)

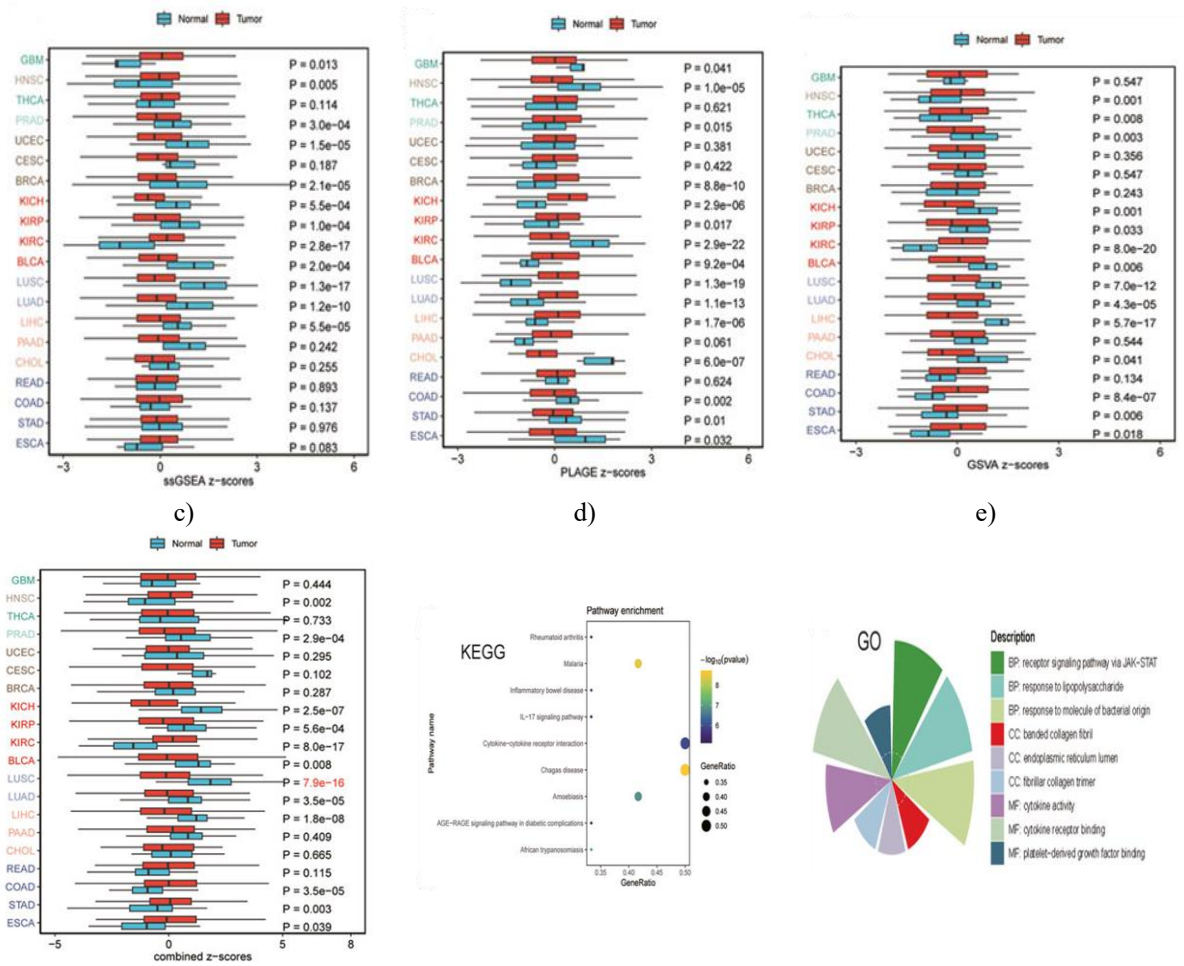

c) d) e)

f) g) h)

Figure 6. Integrated Analysis of Promoter Methylation, Gene Expression, and Pathway Enrichment Across Tumors.

(a) Heatmap depicting promoter methylation differences across multiple cancer types. Rows represent individual genes, and columns correspond to specific cancers. Red indicates higher methylation in tumor tissues relative to normal tissues, while blue reflects lower methylation levels. (b) Heatmap showing the relationship between promoter methylation and mRNA expression across cancers. Each row represents a gene and each column a cancer type. Red denotes a positive correlation, whereas blue indicates a negative correlation, illustrating the complex regulatory effects of methylation on gene expression (c–f) Boxplots comparing pathway activity Z-scores between tumor and normal tissues across various cancers. The vertical axis lists cancer types, and the horizontal axis represents Z-scores for pathway activity. Statistical significance was assessed using the Wilcoxon Rank Sum Test. (g) Scatter plot summarizing KEGG pathway enrichment. Dot size reflects the proportion of genes enriched in each pathway, while the color gradient from yellow to blue indicates significance, with yellow marking the most significant pathways. This visualization highlights key pathways potentially involved in tumor development. (h) Radial plot illustrating Gene Ontology (GO) enrichment. The radius of each segment corresponds to the negative log10 of the adjusted p-value, with larger sectors representing higher enrichment. A gray circle indicates an adjusted p-value of 0.05. This plot emphasizes the most significantly enriched GO terms, revealing critical molecular functions and biological processes altered in cancer.

Anti-inflammatory and antioxidative effects of DHA and EPA on LPS-stimulated RAW 264.7 cells and cancer cells

This study explored the protective effects of the omega-3 fatty acids DHA and EPA against inflammation and cancer cell growth. In LPS-activated RAW 264.7 macrophages, both compounds substantially reduced reactive oxygen species (ROS), as measured by flow cytometry, compared with cells treated with LPS alone **(Figure 7a)**.

Using immunofluorescence, we observed that DHA and EPA markedly suppressed the expression of key inflammatory cytokines, including IL-6 and IL-1β, relative to LPS-stimulated controls **(Figures 7b and 7c)**. This demonstrates their ability to dampen inflammatory signaling at the cellular level.

The impact on cancer cell proliferation was examined through colony formation assays in multiple cell lines (LNCaP, HCT116, HepG2, and A549). Treatment with DHA or EPA resulted in a pronounced reduction in colony numbers, indicating effective inhibition of tumor cell growth **(Figure 7d)**.

Furthermore, the nuclear translocation of SUMO1, a stress-responsive protein, increased under LPS stimulation, but both DHA and EPA reduced its nuclear localization **(Figure 7e)**, suggesting modulation of stress-related signaling pathways.

Taken together, these findings indicate that DHA and EPA act as both antioxidants and anti-inflammatory agents by lowering ROS and downregulating pro-inflammatory cytokines. Their inhibitory effects on cancer cell proliferation and regulation of SUMO1 translocation highlight their potential as therapeutic interventions targeting inflammation and tumor progression.

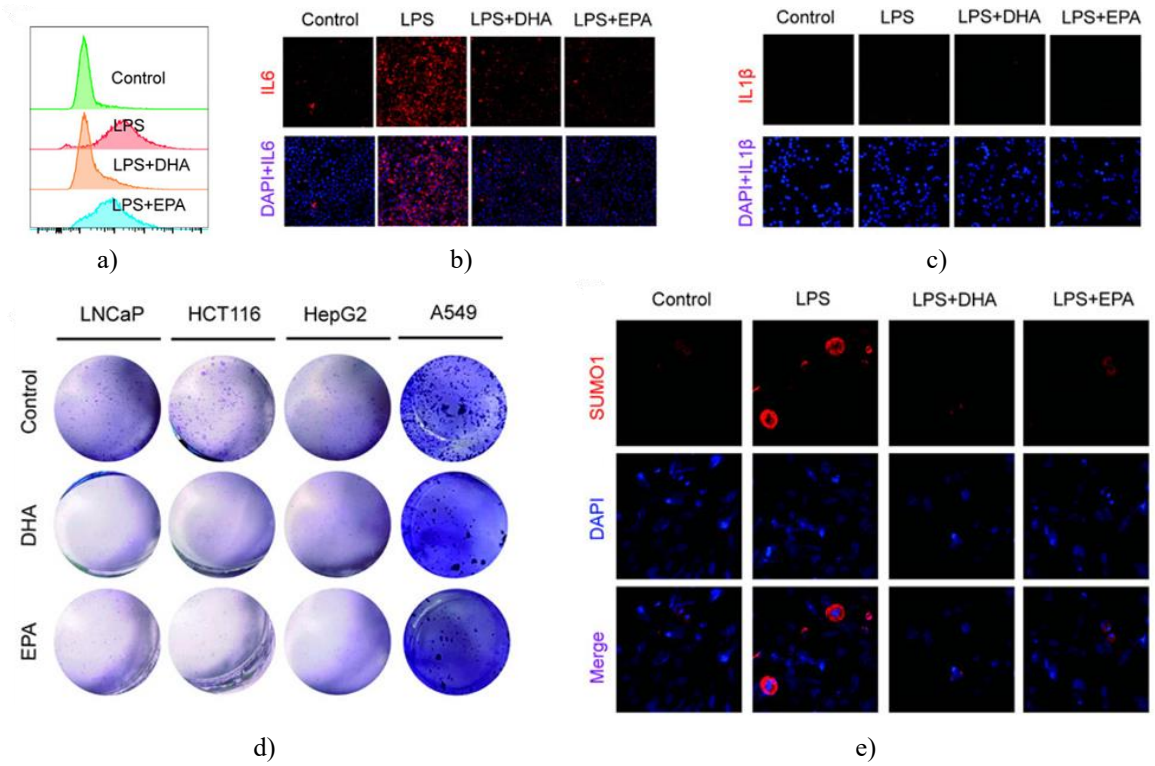

Figure 7.

In this study, we employed two-sample Mendelian randomization (MR) to examine the causal relationships between metabolites and pulmonary hypertension (PH) [17, 18]. Our analyses identified 57 metabolites with significant causal associations to PH. Notably, metabolites such as piperidine, glucuronide, and N-lactoyl-valine showed positive correlations with PH, whereas scoparone (C26) and docosahexaenoic acid (DHA) were negatively associated, suggesting potential protective effects [19]. These findings underscore the metabolic underpinnings of PH and point to specific biochemical pathways that may contribute to its development.

Complementing these findings, pan-cancer genomic analyses revealed substantial alterations in copy number variations, DNA methylation, and tumor mutational burden (TMB) in ASOH genes linked to both PH and various cancers. Genes such as IL6, IL1B, and COL1A1 emerged as central players in gene set enrichment and tumor prediction analyses, highlighting the shared relevance of these genomic perturbations across disease contexts. This overlap suggests that transcriptional changes in metabolically regulated genes may drive genomic alterations in both PH and cancer [20, 21].

The identification of these 57 metabolites strengthens the understanding of PH pathogenesis and offers insights into potential regulatory mechanisms. For instance, phenolic compounds in lentils possess antioxidant properties capable of reducing oxidative stress and alleviating PH symptoms [22-24]. Similarly, studies on arsenic sulphide

in cancer highlight how metabolic substances can influence gene expression through pathways such as HIF-1α/VEGF, drawing parallels with metabolic regulation in PH [25]. Exercise-induced biomarkers also provide a novel perspective on non-pharmacological interventions in PH [26, 27]. Our previous findings on DHA and EPA demonstrate their ability to regulate ROS production and inflammatory cytokines, thereby improving endothelial function and mitigating vascular inflammation.

Certain metabolites, including piperidine glucuronide and N-lactoyl-valine, appear to exacerbate PH, while compounds like scoparone and DHA may act as protective agents and potential therapeutic targets [28, 29]. This aligns with existing literature linking metabolic dysregulation to cardiovascular disease, extending these associations specifically to PH [30, 31]. The pan-cancer analysis further illuminates genomic alterations in overlapping genes, showing interconnected changes in copy number, methylation, and TMB, which are crucial for understanding cancer development and evolution [32, 33]. These findings support a shared inflammatory basis between PH and cancer, particularly involving IL6 and IL1B, while collagen genes such as COL1A1 and COL5A1 highlight extracellular matrix remodeling as a common pathological feature [34, 35].

DHA and EPA effectively attenuate vascular inflammation and remodeling, potentially through modulation of PPAR and NF-κB signaling, thereby improving pulmonary vascular function [36]. Their anti-inflammatory effects may also complement cancer therapies by downregulating pro-tumorigenic cytokines, enhancing the efficacy of chemotherapy and radiotherapy, and reducing treatment-related side effects [37]. Moreover, these omega-3 fatty acids can serve as dietary adjuncts to support immune function and mitigate cachexia in cancer patients [38]. The observed involvement of signaling pathways such as APC/Wnt/β-catenin in both PH and cancer further emphasizes the relevance of these findings for integrated disease management [39, 40].

Despite the comprehensiveness of this study, there are limitations. MR analyses rely on the availability and reliability of genetic instruments, and pleiotropy can confound causal inference [41, 42]. Cohort-specific biases and the use of single-cohort GWAS datasets may limit generalizability, while differences in genetic backgrounds across populations can introduce confounding. Measurement errors in metabolite levels may also attenuate causal estimates. Similarly, pan-cancer analyses may not capture all genetic heterogeneity due to the complexity of tumors [43-45]. Future studies should aim to replicate these findings in larger and more diverse populations to validate the observed mechanisms [46, 47].

Our integrative approach, combining MR and pan-cancer analyses, highlights the interconnected roles of metabolites and genomic alterations in PH and cancer. Understanding these relationships may facilitate the development of targeted therapies that modulate metabolic pathways [48]. Pan-cancer findings also identified potential biomarkers for early cancer detection and prognosis, guiding therapeutic strategies [49, 50]. Studies in network pharmacology and molecular docking, as well as investigations into HER2 and PRMT5 in cancer, support the utility of integrating metabolic and genetic information for precision medicine approaches [51-53]. This multi-faceted approach underscores the value of exploring metabolic-genomic interactions to inform personalized interventions for PH and associated malignancies.

Mechanistically, DHA and EPA were shown to reduce oxidative stress and inflammatory responses in both macrophages and cancer cells, including the nuclear translocation of SUMOylated proteins, which are central to stress and inflammatory signaling [54, 55]. By attenuating oxidative stress, these fatty acids limit SUMO-mediated activation of stress-response genes. SUMOylation also regulates key transcription factors such as NF-κB and STAT1, influencing inflammation and tumor progression [56-58]. Furthermore, SUMOylation modulates tumor suppressors like p53 and HIF-1α, affecting apoptosis and cancer progression, and pharmacological inhibitors targeting SUMO pathways (e.g., TAK-981) are under investigation as anticancer therapies [59, 60]. DHA and EPA may act through similar mechanisms to reduce inflammation, enhance cellular function, and exert anti-tumor effects.

Collectively, these findings deepen clinical understanding of the links between PH and cancer, offering avenues for early diagnostics, biomarker development, and targeted therapies. DHA and EPA demonstrate therapeutic potential by mitigating oxidative stress, inflammation, and vascular remodeling, and future studies should validate these effects in experimental and clinical trials. Integrating multi-omics approaches, including proteomics and transcriptomics, in pan-cancer studies will further elucidate the molecular interplay between metabolites, PH, and cancer, paving the way for innovative interventions and precision medicine strategies.

Conclusion

This study uncovers novel connections between metabolic processes and pulmonary hypertension (PH), while also mapping genomic alterations shared across multiple cancer types. By combining insights from Mendelian randomization with pan-cancer genomic data, the research points to specific metabolites and genes that could serve as actionable biomarkers or targets for therapy. Tailoring treatments based on these molecular signatures has the potential to enhance therapeutic effectiveness and limit adverse effects. Moving forward, validation of these biomarkers in diverse, well-defined patient cohorts is essential. Additionally, large-scale, multicenter clinical studies will be critical to ensure that these findings are broadly applicable across different populations and cancer contexts.

Acknowledgments: We acknowledge the use of ChatGPT-4.0 for grammar and language refinement in this manuscript. No AI involvement occurred in the research content or analysis, and all ethical guidelines were strictly followed.

Conflict of Interest: None

Financial Support: None

Ethics Statement: None

References

1. Cai L, Bai H, Duan J, Wang Z, Gao S, Wang D, et al. Epigenetic alterations are associated with tumor mutation burden in non-small cell lung cancer. J Immunother Cancer. 2019;7:198. doi:10.1186/s40425-019-0660-7
2. Henrichsen CN, Chaignat E, Reymond A. Copy number variants, diseases and gene expression. Hum Mol Genet. 2009;18(R1):R1–R8. doi:10.1093/hmg/ddp011
3. Orozco LD, Cokus SJ, Ghazalpour A, Ingram-Drake L, Wang S, Van Nas A, et al. Copy number variation influences gene expression and metabolic traits in mice. Hum Mol Genet. 2009;18(21):4118–29. doi:10.1093/hmg/ddp360
4. Qi Q, Yang S, Li J, Li P, Du L. Regulation of redox homeostasis through DNA/RNA methylation and post-translational modifications in cancer progression. Antioxid Redox Signal. 2023;39(7–9):531–50. doi:10.1089/ars.2023.0371
5. Ji J, Jing A, Geng T, Ma X, Liu W, Liu B. Editorial: protein modifications in epigenetic dysfunctional diseases: mechanisms and potential therapeutic strategies. Front Cell Dev Biol. 2023;11:1216637. doi:10.3389/fcell.2023.1216637
6. Wang X, Li M. Correlate tumor mutation burden with immune signatures in human cancers. BMC Immunol. 2019;20:4. doi:10.1186/s12865-018-0285-5
7. Filtz TM, Vogel WK, Leid M. Regulation of transcription factor activity by interconnected post-translational modifications. Trends Pharmacol Sci. 2014;35(2):76–85. doi:10.1016/j.tips.2013.11.005
8. Frezza C. Mitochondrial metabolites: undercover signalling molecules. Interface Focus. 2017;7(2):20160100. doi:10.1098/rsfs.2016.0100
9. Schopfer FJ, Cipollina C, Freeman BA. Formation and signaling actions of electrophilic lipids. Chem Rev. 2011;111(10):5997–6021. doi:10.1021/cr200131e
10. Wang Z, Yu T, Huang P. Post-translational modifications of FOXO family proteins (Review). Mol Med Rep. 2016;14(6):4931–41. doi:10.3892/mmr.2016.5867
11. Yao Y, Li H, Da X, He Z, Tang B, Li Y, et al. SUMOylation of Vps34 by SUMO1 promotes phenotypic switching of vascular smooth muscle cells by activating autophagy in pulmonary arterial hypertension. Pulm Pharmacol Ther. 2019;55:38–49. doi:10.1016/j.pupt.2019.01.007
12. Mukherjee D, Lahiri D, Nag M. Therapeutic effects of natural products isolated from different microorganisms in treating cervical cancer: a review. Cancer Insight. 2022;1:31–46. doi:10.58567/ci01020003

13. Liu F, Shi DM, Ma WY, Tang DW, Bai G, Yu XY. Targeting CXCR4 and EDN1 for the treatment of recurrent miscarriage using stearic acid from traditional Chinese medicine. Tradit Med Res. 2024;9:66. doi:10.53388/TMR20240621002
14. Chauleau JY, Trassin M. Sensing multiferroic states non-invasively using optical second harmonic generation. Microstructures. 2024;4. doi:10.20517/microstructures.2023.50
15. Shi FJ, Cai W, Wu N, Li Y. The role of exercise in modulating the HP pathway to reduce glioma-induced epilepsy. Tradit Med Res. 2024;9:73. doi:10.53388/TMR20240309001
16. Jang J, Choi SY. Reduced dimensional ferroelectric domains and their characterization techniques. Microstructures. 2024;4. doi:10.20517/microstructures.2023.67
17. Alhathli E, Julian T, Girach ZUA, Thompson AAR, Rhodes C, Gräf S, et al. A Mendelian randomization study with clinical follow-up links metabolites to risk and severity of pulmonary arterial hypertension. J Am Heart Assoc. 2023;13:e032256. doi:10.1101/2023.06.30.23292100
18. Wang Z, Chen S, Zhu Q, Wu Y, Xu G, Guo G, et al. Using a two-sample Mendelian randomization method in assessing the causal relationships between human blood metabolites and heart failure. Front Cardiovasc Med. 2021;8:695480. doi:10.3389/fcvm.2021.695480
19. Re K, Gandhi J, Liang R, Patel S, Joshi G, Smith NL, et al. Clinical utility of ozone therapy and hyperbaric oxygen therapy in degenerative disc disease. Med Gas Res. 2023;13(1):1–6. doi:10.4103/2045-9912.351890
20. Thakur C, Chen F. Connections between metabolism and epigenetics in cancers. Semin Cancer Biol. 2019;57:52–8. doi:10.1016/j.semcancer.2019.06.006
21. Ibrahim S, Muhammad F. Cancer aetiology and progression: the crucial link between genome, epigenome and metabolome. Niger J Basic Clin Sci. 2020;17(2):77. doi:10.4103/njbcs.njbcs_2_20
22. Xia M, Li M, De Souza TSP, Barrow C, Dunshea FR, Suleria HAR. LC-ESI-QTOF-MS2 characterization of phenolic compounds in different lentil (Lens culinaris M.) samples and their antioxidant capacity. Front Biosci (Landmark Ed). 2023;28:44. doi:10.31083/j.fbl2803044
23. Park YR, Kwon SJ, Kim JH, Duan S, Eom SH. Light-induced antioxidant phenolic changes among the sprouts of lentil cultivar. Antioxidants (Basel). 2024;13(4):399. doi:10.3390/antiox13040399
24. Żuchowski J, Rolnik A, Adach W, Stochmal A, Olas B. Modulation of oxidative stress and hemostasis by flavonoids from lentil aerial parts. Molecules. 2021;26(2):497. doi:10.3390/molecules26020497
25. Lu S, Cai Y, Kang T, Zhu C, Feng Z, Chen S. Arsenic sulfide inhibits hepatocellular carcinoma metastasis by suppressing the HIF-1α/VEGF pathway. Front Biosci (Landmark Ed). 2023;28:152. doi:10.31083/j.fbl2807152
26. Yau SY, Li A, Sun X, Fontaine CJ, Christie BR, So KF. Potential biomarkers for physical exercise-induced brain health. In: Wang M, Witzmann FA, editors. Role of biomarkers in medicine. Rijeka: InTech; 2016. doi:10.5772/62458
27. Reis VM. Effects of exercise on biomarkers in health and disease: some new insights with special focus on extreme exercise and healthy ageing. Int J Environ Res Public Health. 2020;17(6):1986. doi:10.3390/ijerph17061986
28. Li Y, Zhao X. NMR-based plasma metabonomics in hyperlipidemia mice. Anal Methods. 2020;12(15):1995–2001. doi:10.1039/D0AY00487A
29. Chen T, Yuan H, Sun YB, Song YC, Lu M, Ni X, et al. Metabolomics study of the prefrontal cortex in a rat model of attention deficit hyperactivity disorder reveals the association between cholesterol metabolism disorder and hyperactive behavior. Biochem Biophys Res Commun. 2020;523(2):315–21. doi:10.1016/j.bbrc.2019.12.016
30. Chan SY, Rubin LJ. Metabolic dysfunction in pulmonary hypertension: from basic science to clinical practice. Eur Respir Rev. 2017;26(143):170094. doi:10.1183/16000617.0094-2017
31. Harvey L, Chan S. Emerging metabolic therapies in pulmonary arterial hypertension. J Clin Med. 2017;6(4):43. doi:10.3390/jcm6040043
32. Thomson JP, Meehan RR. DNA methylation changes in cancer. In: Kaneda A, Tsukada Y, editors. DNA and histone methylation as cancer targets. Cham: Springer; 2017. p. 75–96. doi:10.1007/978-3-319-59786-7_4
33. Chen C, Wang Z, Ding Y, Wang L, Wang S, Wang H, et al. DNA methylation: from cancer biology to clinical perspectives. Front Biosci (Landmark Ed). 2022;27:326. doi:10.31083/j.fbl2712326

34. Dzobo K, Leaner VD, Parker MI. Feedback regulation of the α2(1) collagen gene via the Mek–Erk signaling pathway. IUBMB Life. 2012;64(2):87–98. doi:10.1002/iub.568
35. Machol K, Polak U, Weisz-Hubshman M, Song IW, Chen S, Jiang MM, et al. Molecular alterations due to Col5a1 haploinsufficiency in a mouse model of classic Ehlers–Danlos syndrome. Hum Mol Genet. 2022;31(8):1325–35. doi:10.1093/hmg/ddab323
36. Łacheta D, Olejarz W, Włodarczyk M, Nowicka G. Effect of docosahexaenoic acid (DHA) and eicosapentaenoic acid (EPA) on the regulation of vascular endothelial cell function. Postepy Hig Med Dosw (Online). 2019;73:467–475. doi:10.5604/01.3001.0013.5064
37. Silva JAP, Fabre MES, Waitzberg DL. Omega-3 supplements for patients in chemotherapy and/or radiotherapy: a systematic review. Clin Nutr. 2015;34(3):359–66. doi:10.1016/j.clnu.2014.11.005
38. Szlendak M, Kapała A. Does the ratio of eicosapentaenoic acid to docosahexaenoic acid matter in cancer treatment? A systematic review of their effects on cachexia-related inflammation. Nutrition. 2024;124:112466. doi:10.1016/j.nut.2024.112466
39. De Jesus Perez VA, Yuan K, Orcholski ME, Sawada H, Zhao M, Li CG, et al. Loss of adenomatous polyposis coli–α3 integrin interaction promotes endothelial apoptosis in mice and humans. Circ Res. 2012;111(12):1551–64. doi:10.1161/CIRCRESAHA.112.267849
40. Billmann M, Chaudhary V, ElMaghraby MF, Fischer B, Boutros M. Widespread rewiring of genetic networks upon cancer signaling pathway activation. Cell Syst. 2018;6(1):52–64. doi:10.1016/j.cels.2017.10.015
41. LaPierre N, Fu B, Turnbull S, Eskin E, Sankararaman S. Leveraging family data to design Mendelian randomization that is provably robust to population stratification. bioRxiv. 2023. doi:10.1101/2023.01.05.522936
42. Slob EAW, Burgess S. A comparison of robust Mendelian randomization methods using summary data. Genet Epidemiol. 2020;44(4):313–29. doi:10.1002/gepi.22295
43. Tan H, Bao J, Zhou X. Genome-wide mutational spectra analysis reveals significant cancer-specific heterogeneity. Sci Rep. 2015;5:12566. doi:10.1038/srep12566
44. Raynaud F, Mina M, Tavernari D, Ciriello G. Pan-cancer inference of intra-tumor heterogeneity reveals associations with different forms of genomic instability. PLoS Genet. 2018;14(9):e1007669. doi:10.1371/journal.pgen.1007669
45. Nakamura K, Aimono E, Tanishima S, Imai M, Nagatsuma AK, Hayashi H, et al. Intratumoral genomic heterogeneity may hinder precision medicine strategies in patients with serous ovarian carcinoma. Diagnostics (Basel). 2020;10(4):200. doi:10.3390/diagnostics10040200
46. Melamud E, Taylor DL, Sethi A, Cule M, Baryshnikova A, Saleheen D, et al. The promise and reality of therapeutic discovery from large cohorts. J Clin Invest. 2020;130(2):575–81. doi:10.1172/JCI129196
47. Frank J, Ruggiero ED, McInnes RR, Kramer M, Gagnon F. Large life-course cohorts for characterizing genetic and environmental contributions: the need for more thoughtful designs. Epidemiology. 2006;17(5):595–8. doi:10.1097/01.ede.0000239725.48908.7d
48. Kaddurah-Daouk R, Weinshilboum RM; Pharmacometabolomics Research Network. Pharmacometabolomics: implications for clinical pharmacology and systems pharmacology. Clin Pharmacol Ther. 2014;95(2):154–67. doi:10.1038/clpt.2013.217
49. Ding W, Chen G, Shi T. Integrative analysis identifies potential DNA methylation biomarkers for pan-cancer diagnosis and prognosis. Epigenetics. 2019;14(1):67–80. doi:10.1080/15592294.2019.1568178
50. Ibrahim J, Op De Beeck K, Fransen E, Peeters M, Van Camp G. Genome-wide DNA methylation profiling and identification of potential pan-cancer and tumor-specific biomarkers. Mol Oncol. 2022;16(12):2432–47. doi:10.1002/1878-0261.13176
51. Cao Y, Wang C, Dong L. Exploring the mechanism of white peony in the treatment of lupus nephritis based on network pharmacology and molecular docking. Arch Esp Urol. 2023;76(2):123–31. doi:10.56434/j.arch.esp.urol.20237602.13
52. Li Q, Su X, Qing L, Xu W, Yang Y, You C, et al. HER2 affects the biological behaviours of bladder cancer cells and is closely associated with the progression and prognosis of bladder cancer. Arch Esp Urol. 2024;77(1):79–91. doi:10.56434/j.arch.esp.urol.20247701.11
53. Huang L, Zhang XO, Rozen EJ, Sun X, Sallis B, Verdejo-Torres O, et al. PRMT5 activates AKT via methylation to promote tumor metastasis. Nat Commun. 2023;14:3955. doi:10.1038/s41467-022-31645-1

54. Guo C, Henley JM. Wrestling with stress: roles of protein SUMOylation and deSUMOylation in cell stress response. IUBMB Life. 2014;66(2):71–7. doi:10.1002/iub.1244
55. Pascual G, Fong AL, Ogawa S, Gamliel A, Li AC, Perissi V, et al. A SUMOylation-dependent pathway mediates transrepression of inflammatory response genes by PPAR-gamma. Nature. 2005;437(7059):759–63. doi:10.1038/nature03988
56. Parra-Peralbo E, Muratore V, Barroso-Gomila O, Talamillo A, Sutherland JD, Barrio R. Role of sumoylation in neurodegenerative diseases and inflammation. In: Proteostasis and proteolysis. Boca Raton: CRC Press; 2021. 95–106. doi:10.1201/9781003048138-08
57. Yang Q, Tang J, Xu C, Zhao H, Zhou Y, Wang Y, et al. Histone deacetylase 4 inhibits NF-κB activation by facilitating IκBα sumoylation. J Mol Cell Biol. 2021;12(12):933–45. doi:10.1093/jmcb/mjaa043
58. Decque A, Joffre O, Magalhaes JG, Cossec JC, Blecher-Gonen R, Lapaquette P, et al. Sumoylation coordinates the repression of inflammatory and anti-viral gene-expression programs during innate sensing. Nat Immunol. 2016;17(2):140–9. doi:10.1038/ni.3342
59. Lee JS, Choi HJ, Baek SH. Sumoylation and its contribution to cancer. Adv Exp Med Biol. 2017;963:283–98. doi:10.1007/978-3-319-50044-7_17
60. Kukkula A, Ojala VK, Mendez LM, Sistonen L, Elenius K, Sundvall M. Therapeutic potential of targeting the SUMO pathway in cancer. Cancers (Basel). 2021;13(17):4402. doi:10.3390/cancers13174402